



Measurement of cross section of (n, γ) reaction for, iodine, sodium and vanadium in the energy range 1 keV to 4 MeV using accelerator based neutron source



M.S. Barough^a, B.J. Patil^{a,b}, V.N. Bhoraskar^a, S.D. Dhole^{a,*}

^a Department of Physics, University of Pune, Pune 411 007, India

^b Abasaheb Garware College, Karve Road, Pune 411 004, India

ARTICLE INFO

Article history:

Received 27 November 2012

Received in revised form 19 March 2013

Accepted 21 March 2013

Available online 21 April 2013

Keywords:

Cross section

Neutron source

Activation analysis

FLUKA

TALYS

EMPIRE

ABSTRACT

The cross sections of $^{127}\text{I}(n, \gamma)^{128}\text{I}$, $^{23}\text{Na}(n, \gamma)^{24}\text{Na}$ and $^{51}\text{V}(n, \gamma)^{52}\text{V}$ reactions for iodine, sodium and vanadium were measured at continuous energy spectrum using a Microtron accelerator based neutron source. In this case, the bremsstrahlung radiation emitted by impinging 6 MeV electrons on the e- γ primary target (tungsten) was allowed to fall on the γ -n secondary target (beryllium) to produce continuous neutrons. The optimization of bremsstrahlung and neutron producing targets along with their spectra were estimated using FLUKA code. The cross sections of $^{127}\text{I}(n, \gamma)^{128}\text{I}$, $^{23}\text{Na}(n, \gamma)^{24}\text{Na}$ and $^{51}\text{V}(n, \gamma)^{52}\text{V}$ reactions over the neutron energy from 1 keV to 4 MeV have been also calculated using the TALYS-1.2 and EMPIRE nuclear model codes. The variations of the cross sections with the level densities and effective imaginary potentials were studied to obtain the best fit of the excitation function. It is observed that the experimental cross sections for iodine, sodium and vanadium are in good agreement with the TALYS-1.2 and EMPIRE codes.

© 2013 Elsevier Ltd. All rights reserved.

1. Introduction

Neutron activation cross-section data is very important for theoretical and experimental studies by concerning the interaction of neutrons with matter. It is obvious that the cross-section data of the nuclear reactions induced by different energy neutrons are required for several applications in the areas of applied nuclear physics, nuclear models, elemental analysis, reactor technology, etc. In recent years, there have been rapid growth of low and medium energy electron accelerator based neutron sources for medical and industrial applications because of their compactness, easy handling, adjustable flux, no radioactive waste, less shielding requirement, etc. However, very few attempts have been made to use these kinds of accelerators based neutron source for nuclear reaction studies.

Iodine is considered as one of the fission products (FPs) that might be generated in the core of light water reactors and is recognized as the most relevant to public health consequences in case of an accident with the environmental release of FPs (Moriyama et al., 2010). The recoil study of hot iodine in iodocompounds is less perplexing because of its mono-isotopic nature (Dicksic et al., 1976). A high thermal neutron capture cross section ($6.2 \pm 0.26b$) of iodine

(Zaman et al., 2011) and convenient half life (25 min) of ^{128}I enable researchers to study favorably the high energy iodine chemistry following $^{127}\text{I}(n, \gamma)^{128}\text{I}$ reaction. Moreover, the characteristics of ^{128}I compound nucleus and its subsequent de-excitation through photon emission or electron conversion and the associated recoil spectra (Yoong et al., 1972) have made the subject interesting. The spin and parity i.e. 1^+ (Schaller et al., 1971) of the ground state of ^{128}I is different from the spin and parity of ^{127}I i.e. $5/2^+$ (Rustgi et al., 1968). These characteristics are much beneficial in evaluating and understanding the (n, γ) consequences in iodine containing compounds. One of the earlier studies on the production of ^{128}I is due to (Benczer et al., 1956). Maruyama and Idenawa also produced ^{128}I atoms by small research reactor (Maruyama and Idenawa, 1967).

Sodium is used as a coolant material in fast reactors and thus its neutron nuclear data are important. The neutron nuclear data for ^{23}Na has already been studied by various researchers based on the experimental as well as theoretical predictions. On the other hand vanadium is thought to be a promising structural material for the use in high temperature neutronic system, especially where tritium is a concern material.

Keeping the importance of ^{128}I , ^{24}Na , ^{52}V elements in nuclear reactor as a high level radioactive waste, cooling and structural materials the (n, γ) reaction cross-section have been experimentally measured using the accelerator based neutron source. In the present experiment, the bremsstrahlung radiation emitted by

* Corresponding author.

E-mail address: sanjay@physics.unipune.ac.in (S.D. Dhole).

impinging 6 MeV electrons on the $e\text{-}\gamma$ target are allowed to fall on the $\gamma\text{-n}$ target to produce neutrons. These neutrons have continuous energy spectrum and has been used for the present experiment. The cross sections measured in this work have been compared with the literature values from the EXFOR database, and with theoretical model calculations using the TALYS-1.2 and EMPIRE nuclear model codes.

2. Experimental details

2.1. Experimental setup

For the present work, a 6 MeV Race-Track Microtron accelerator based neutron source from the Department of Physics, University of Pune was used. The Microtron, (Bhoraskar, 1988) is a re-circulating electron accelerator in which an electron beam repeatedly passed through RF accelerating cavity (Asgekar et al., 1980). The Microtron was operated at a particular energy of 6 MeV electron beam. Pulsed current of the electron beam was 1–10 mA having pulse width 2.0 μs and pulse rate 50 pps. Electron beam current was measured by using faraday cup arrangement. Hence, the average current of the electron beam was varied between 0.1 and 1 μA . The 6 MeV energy electrons beam was bombarded on tungsten target to produce bremsstrahlung radiation, which interacts with beryllium target to gives continuous energy neutrons. In the present work, beryllium is chosen as the $\gamma\text{-n}$ target since it has three peaks of photo-production cross section in the region below 3 MeV, and the product nuclei ${}^8\text{Be}$ quickly (10^{-16} s) decays into stable ${}^4\text{He}$ atoms. Usually, neutrons are formed in interactions of photons with beryllium nucleus through ${}^9\text{Be}(\gamma, n){}^8\text{Be}$ reaction. Thus the tungsten ($e\text{-}\gamma$ target) was used as an electron to $\gamma\text{-ray}$ convertor, whereas beryllium ($\gamma\text{-n}$ target) was used as a $\gamma\text{-ray}$ to neutron convertor. Fig. 1 shows the experimental setup for the measurement of cross section of (n, γ) reactions. During the experiment, the collimated beam of bremsstrahlung radiation was used to impinge on the beryllium target to produce neutrons

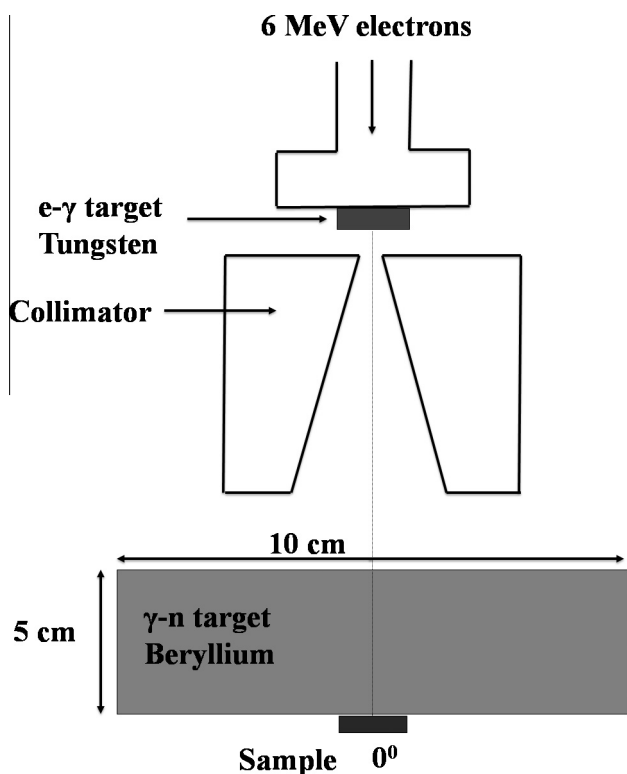


Fig. 1. Experimental setup for the measurement of nuclear reaction cross sections.

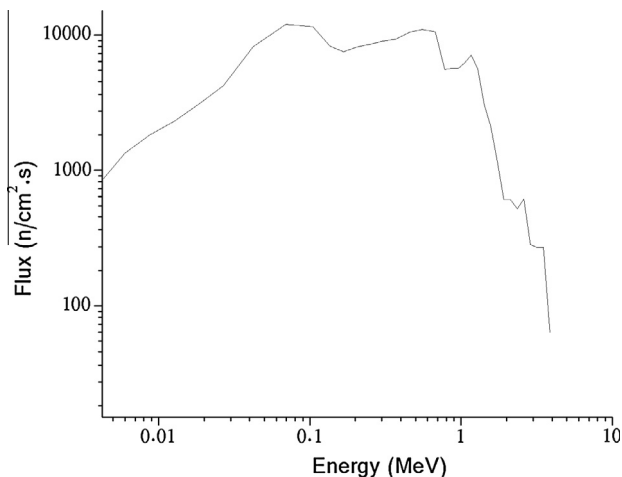


Fig. 2. Neutron spectra from the Microtron accelerator based neutron source (simulated by FLUKA).

isotropically. The angular distributions of these neutrons have been measured (Patil et al., 2010) and the maximum neutron flux observed to be in the forward direction. Therefore, for the present experiment sample of which the (n, γ) reaction cross section to be measured was kept at 0° . The experimental setup shown in Fig. 1 was designed in FLUKA and estimated the neutron energy spectrum at the target. The neutron energy spectrum estimated at 0° in FLUKA is shown in Fig. 2. It is observed from the figure that the continuous neutron energies coming out from the beryllium and estimated at the sample are ranging from 1 keV to 4 MeV. The total neutron flux is around to be 1.0×10^4 n/cm² s.

2.2. Samples

In this work, powders of pure chemical compound of iodine (I_4O_9 powder 99% purity), sodium (NaCl powder 99% purity) and vanadium (V_2O_5 powder 99% purity) were used. Each sample was made by packing a known weight in a polyethylene bag. The size of each sample was $\sim 6\text{cm} \times \sim 3\text{cm}$ and $\sim 1\text{cm}$ thick.

2.3. Neutron irradiation and cross section calculations

Each sample was mounted on faraday cup and was irradiated with the experimental setup shown in Fig. 1 for the measurement of nuclear reaction cross sections. The electron beam having energy 6 MeV was allowed to fall on the primary cylindrical tungsten target ($r = 0.3\text{cm}$ and thickness = 0.22 cm) and generated bremsstrahlung radiations. The tungsten target was mounted on the extraction window of the Microtron accelerator. Further, these bremsstrahlung radiations were made to fall on the secondary beryllium target having dimensions $10\text{cm} \times 10\text{cm} \times 5\text{cm}$, which generated neutrons through the (γ, n) reaction. After neutron irradiation, each sample was removed from the faraday cup and was then taken it to the high purity germanium (HPGe) detector based gamma-ray spectroscopy for the measurement of induced gamma activity. The HPGe detector was calibrated using standard gamma sources. The measured gamma spectrum was analyzed by the GENIE2K software based multichannel analyzer (MCA). The achieved count rate can be used to determine activation integrals and other parameters of the nuclear reactions by making necessary corrections. The details of the energies and branching of the γ rays adopted in the cross-section estimation, the irradiation time, cooling time, and counting time are given in Table 1.

From the gamma ray activity of the reaction products such as ${}^{128}\text{I}$, ${}^{24}\text{Na}$ and ${}^{52}\text{V}$ their ${}^{127}\text{I}(n, \gamma)$, ${}^{23}\text{Na}(n, \gamma)$ and ${}^{51}\text{V}(n, \gamma)$ reaction

Table 1

Nuclear reactions, with along their corresponding decay data of half life, energies, gamma intensity, irradiation time, cooling time, and counting time.

Reaction	Half-life of reaction products	γ Energy (MeV)	γ Intensity (%)	Irradiation time (s)	Cooling time (s)	Counting time (s)
$^{51}\text{V}(n, \gamma)^{52}\text{V}$	3.75 m	1.434	100	600	30	637.34
$^{23}\text{Na}(n, \gamma)^{24}\text{Na}$	14.96 h	1.369	100	1200	30	7200
		2.754	100			
$^{127}\text{I}(n, \gamma)^{128}\text{I}$	24.99 m	0.441	14	2100	30	1800
		0.528	1.4			
		0.743	0.2			
		0.969	0.3			

cross-sections were estimated by using the following activation relation (Curtiss, 1969),

$$\sigma = \frac{A_i \lambda}{\phi \beta N \varepsilon (1 - e^{-\lambda t_1}) e^{-\lambda t_2} (1 - e^{-\lambda t_3})} \quad (1)$$

where ϕ is the incident neutron flux, σ is the cross section for (n, γ) reaction, A_i is the total number of counts, λ is the decay constant, β is the number of gamma quanta/disintegration, N is the number of atoms in the target; ε is the efficiency of the detector (0.06), t_1 is the irradiation time, t_2 is the cooling time, i.e., the time between end of irradiation and start of counting, t_3 is the counting time. Energy resolution of detector (at 1.33 MeV) is 1.4 keV. However, in the present case continuous neutron energy spectrum was used for the measurement of neutron reaction cross section.

Therefore, the equation for continuous neutron energy can be written as

$$\sum_{j=1}^{j=n} \sigma_j \phi_j = \frac{A_i \lambda}{\beta N \varepsilon (1 - e^{-\lambda t_1}) e^{-\lambda t_2} (1 - e^{-\lambda t_3})} \quad (2)$$

where j run from first energy bin to last energy bin (1–n).

The average cross section, $\bar{\sigma}$, over an interval, is the integral of the cross section multiplied by the flux divided by the integrated flux, which can be written as

$$\bar{\sigma} = \frac{\int_{E_1}^{E_2} \sigma(E) \phi(E) dE}{\int_{E_1}^{E_2} \phi(E) dE} \quad (3)$$

This equation in terms of summation can be written as

$$\bar{\sigma} = \frac{\sum_{j=1}^{j=n} \sigma_j \phi_j}{\sum_{j=1}^{j=n} \phi_j} \quad (4)$$

$$\bar{\sigma} = \frac{A_i \lambda}{\beta N \varepsilon (1 - e^{-\lambda t_1}) e^{-\lambda t_2} (1 - e^{-\lambda t_3}) \varphi_{\text{integrated}}} \quad (5)$$

$$\bar{\sigma} = \frac{A_i \lambda}{\varphi_{\text{integrated}} \beta N \varepsilon (1 - e^{-\lambda t_1}) e^{-\lambda t_2} (1 - e^{-\lambda t_3})} \quad (6)$$

Using Eq. (6), we determine the experimental average cross section for iodine, sodium and vanadium at continuous energy spectra of neutron.

3. Theoretical calculations

In this work, the cross sections for the formation of ^{128}I , ^{24}Na and ^{52}V through the, $^{127}\text{I}(n, \gamma)^{128}\text{I}$, $^{23}\text{Na}(n, \gamma)^{24}\text{Na}$ and $^{51}\text{V}(n, \gamma)^{52}\text{V}$ reactions over the neutron energy range from 1 keV to 4 MeV have been calculated using the TALYS-1.2 and EMPIRE nuclear model codes. The nuclear structure database has been generated from the Reference Input Parameter Library, RIPL (Capote et al., 2009) and that is used as a basis for TALYS. Optical model potentials (OMPs) used in TALYS are the local and global parameterisations of Koning and Delaroche (2003). The microscopic combinatorial model has been proposed by Goriely et al. (2008).

Gamma-ray transmission coefficients enter the Hauser–Feshbach model for the calculation of the competition of photons with other particles. In addition, the two component exciton model by Kalbach (1986) are applied for pre-equilibrium calculations.

The calculations have been carried out using different choices of the level density parameters obtained from the Fermi gas model as well as from Goriely's table (Goriely et al., 2008). The discrete energy level scheme has been adopted from the Reference Input Parameters Library (RIPL-2) and as such 25 discrete levels are considered to be below 2 MeV energy. For the RIPL database (Goriely et al., 2008), Goriely has calculated level densities from drip line to drip line on the basis of Hartree–Fock calculations, covering excitation energies up to 150 MeV and spin values l up to 30 (Koning et al., 2004).

The EMPIRE, statistical model code for the nuclear reaction has also been used for calculating the cross-sections for formation of ^{128}I , ^{24}Na and ^{52}V respectively and the respective compound nucleus model are employed. The optical model parameters of Koning et al. (2004) for neutrons (Lib. No. 1430) and protons (Lib. No. 4426) used in this work have been extracted from the Reference Input Parameter Library (RIPL-2) developed at IAEA. The level densities calculated using dynamic approach, specific to the EMPIRE code, in which the collective enhancements of the level densities due to the nuclear vibrations and rotations are considered.

Level densities are calculated using the following expression

$$\rho(U, J) = \rho_{\text{BCS}}(U, J) Q_{\text{rot}}^{\text{BCS}} K_{\text{rot}} Q_{\text{vib}} K_{\text{vib}} \quad (7)$$

where K_{vib} is the vibrational enhancement and Q_{vib} is its damping. K_{rot} is the rotational enhancement and Q_{rot} is its damping. $\rho_{\text{BCS}}(U, J)$ is the super fluid model (BCS) level densities (Ignatyuk et al., 1979) are calculated according to the expression

$$\rho_{\text{BCS}}(U, J) = \frac{2J+1}{2\sqrt{2\pi}\sigma_{\text{eff}}^3 \sqrt{\text{Det}}} \exp\left(\frac{S-J(J+1)}{2\sigma_{\text{eff}}^2}\right) \quad (8)$$

where σ_{eff} is the effective spin cut-off factor, S is the entropy of system, J is the nuclear spin and U is the excitation energy after making the pairing correction.

The low-energy part of level densities is calculated in terms of the super-fluid models when EMPIRE specific parameterization of the level density parameter 'a' is selected (Ignatyuk et al., 1979). Parameter 'a' is assumed

$$a(U) = \tilde{a} \left[1 + f(U) \frac{\delta w}{U} \right] \quad (9)$$

where δw is the shell correction and \tilde{a} is the asymptotic value of a parameter and $f(U) = \exp(-\gamma U)$ With the pairing gap $\Delta = 12/(A)^{1/2}$ the critical temperature T_{crit} is

$$T_{\text{crit}} = 0.567\Delta \quad (10)$$

4. Nuclear models

The excitation functions for the reactions have been studied theoretically by using the nuclear model code TALYS-1.2 (Koning et al., 2004). The optical model parameters for neutrons and

protons are obtained by a local potential proposed by Koning and Delaroche (2003). The compound nucleus contribution is calculated by the Hauser–Feshbach model (Hauser and Feshbach, 1952). The two-component exciton model developed by Kalbach (1986) is used for calculating the pre-equilibrium contribution.

The optical model potentials for neutrons and protons used in the TALYS-1.2 nuclear model code are the global parametrizations given by Koning and Delaroche (2003). These optical potentials by Koning and Delaroche have been tested for $12 < A < 339$ in the energy range 1 keV to 200 MeV. However, the simple folding approach for alpha particles used by Watanabe (1958). In the nuclear reactions involving projectiles and ejectiles with different proton and neutron numbers, the processes such as stripping, pick-up, and knockout play important roles in deciding the cross sections. The direct-like reactions are not entirely covered by the exciton model (Koning et al., 2004). To include the effects of these processes, the phenomenological theory developed by Kalbach (1986) has been added in the TALYS-1.2 nuclear model code. In the two-component exciton model, the creation of neutron and proton type particles and holes are explicitly followed throughout the reaction.

By applying five different choices of the level density model available in TALYS-1.2, the level density parameters have been calculated. The theoretical calculations have been carried out using the default parameter values with the only change being made in the choice of the level density models. The statistical model used in the EMPIRE is an advanced implementation of the Hauser–Feshbach theory. The exact angular momentum and parity coupling is observed. The emission of neutrons, protons is taken into account along with the competing fission channel. The full gamma-cascade in the residual nuclei is considered. Particular attention is dedicated to the determination of the level densities, which can be calculated in the non-adiabatic approach allowing for the rotational and vibrational enhancements. These collective effects are gradually removed above certain energy. Level densities acquire dynamic features though the dependence of the rotational enhancement on the shape of a nucleus.

The emission of gamma in the Multistep Compound (MSC) mechanism is treated in terms of the model proposed by Hoering and Weidenmuller (1992). The model assumes that gamma emission occurs through the de-excitation of the Giant Dipole Resonance (GDR) built within classes. Following Brink-Axel hypothesis (Brink, 1957) each nuclear state serves as the basis of a GDR excitation with identical properties.

5. Results and discussion

The cross sections for the formation of ^{128}I , ^{24}Na and ^{52}V through the $^{127}\text{I}(n, \gamma)^{128}\text{I}$, $^{23}\text{Na}(n, \gamma)^{24}\text{Na}$ and $^{51}\text{V}(n, \gamma)^{52}\text{V}$ reactions induced by 1 keV to 4 MeV neutrons have been theoretically estimated using TALYS-1.2 and EMPIRE nuclear model codes. The cross sections are mainly studied by (i) different level density parameters, (ii) varying the effective imaginary potentials, and (iii) incorporating contributions of the negative parity energy levels. From the decay scheme of ^{24}Na shown in Fig. 3, it is observed that ^{24}Na nuclei can decay from the positive parity energy level 1.35 MeV (1+) to a metastable state 0.473 MeV (1+) by gamma emission with half-life 0.02 s. Similarly, ^{24}Mg nuclei can decay from the positive parity energy level 2.754 MeV (4+) to a metastable state 1.368 MeV (2+) by gamma emission involving E2 transition with 100% decay probability. Moreover, ^{24}Mg nuclei can decay from the positive parity metastable state 1.368 MeV (2+) to stable by gamma emission involving E2 transition with 100% decay probability. During the experiment, activity of 0.473 MeV gamma-ray due to ^{24m}Na was observed. Fig. 4 shows

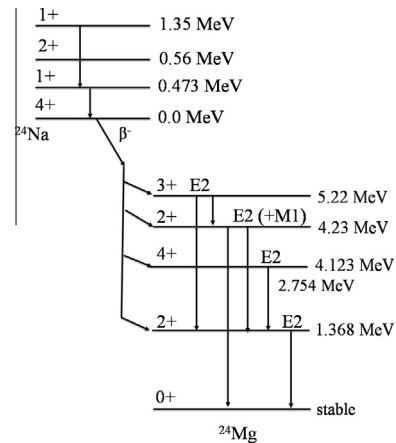


Fig. 3. Decay scheme of ^{24}Na and ^{24}Mg nuclei.

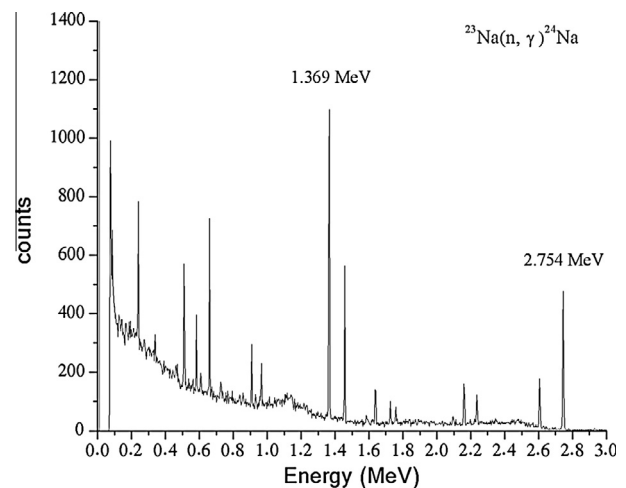


Fig. 4. Gamma-ray spectrum of ^{24}Na produced through $^{23}\text{Na}(n, \gamma)^{24}\text{Na}$ reaction induced by continuous neutron energy.

a gamma-ray spectrum of the ^{23}Na irradiated with continuous neutron energy up to 4 MeV in which photo-peaks at 0.473 MeV due to ^{24m}Na and another peaks at 1.368 MeV and 2.754 MeV are also clearly observed. From the decay scheme of $^{24}\text{Na}^*$, shown in Fig. 3, it is clear that the 0.473 MeV gamma-ray is emitted in the decay of ^{24}Na from the metastable state to ground state. These results, therefore, indicate that ^{24}Na can be produced through $^{23}\text{Na}(n, \gamma)^{24}\text{Na}$ reaction induced by continuous neutron energy up to 4 MeV.

Fig. 5 shows the excitation function for the reaction $^{23}\text{Na}(n, \gamma)^{24}\text{Na}$ over the continuous neutron energy up to 4 MeV using EMPIRE and TALYS-1.2 nuclear model codes. From Fig. 5, it has been observed that the experimental results are in agreement with the literature data of Bame et al. (1959) and ENDF/B-VII.1 (2011). But the present experimental values are not in coincident with TALYS-1.2 and EMPIRE, even though the results are based on the best possible results of TALYS-1.2 and EMPIRE to meet the experimental values.

From the decay scheme shown in Fig. 6, it is observed that ^{52}V with half-life 3.76 min has β^- decay and ^{52}Cr nuclei having half-life 0.7 ps can decays from the positive parity metastable state 1.434 MeV (2+) to stable state by the gamma emission with 100% decay probability. Fig. 7 shows a gamma-ray spectrum of the ^{51}V irradiated with continuous neutron energy up to 4 MeV in which photo-peak at 1.434 MeV is clearly observed. These results,

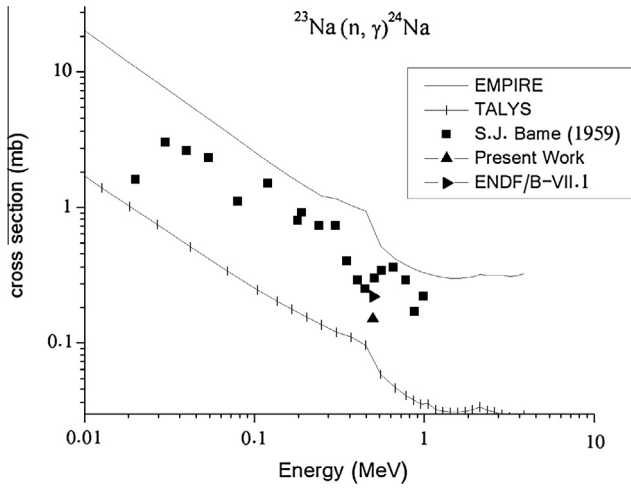


Fig. 5. Experimental and theoretical cross-sections for $^{23}\text{Na}(n, \gamma)^{24}\text{Na}$ reaction.

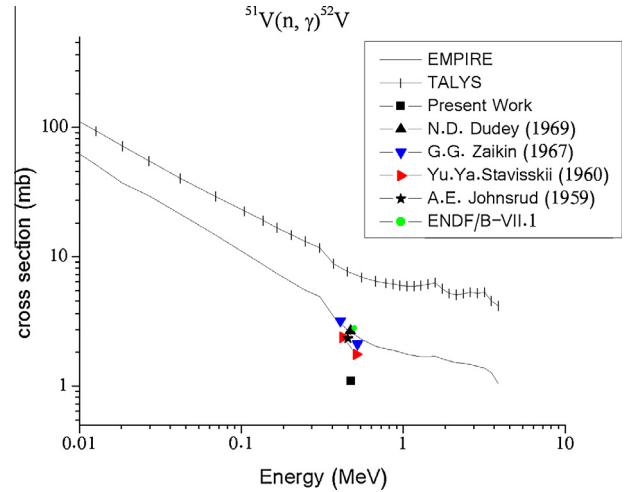


Fig. 8. Measured and theoretical cross-sections for $^{51}\text{V}(n, \gamma)^{52}\text{V}$ reaction uses EMPIRE and TALYS.

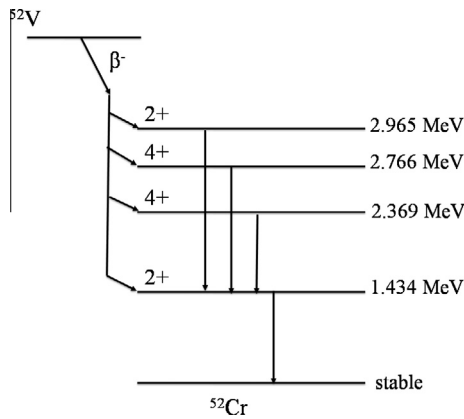


Fig. 6. Decay scheme of ^{52}V and ^{52}Cr nuclei.

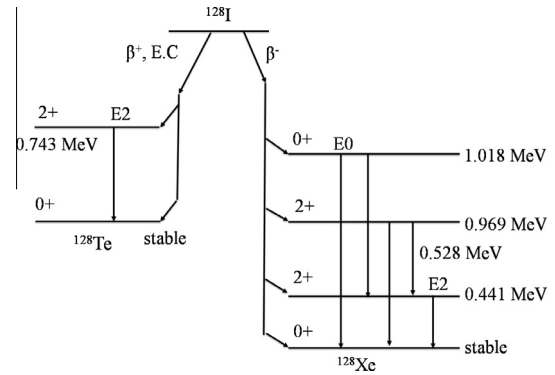


Fig. 9. Decay scheme of ^{128}I , ^{128}Xe and ^{128}Te nuclei.

therefore, indicate that ^{52}Cr can be produced through $^{51}\text{V}(n, \gamma)^{52}\text{V}$ reaction induced by continuous neutron energy up to 4 MeV.

Fig. 8 shows the measured and theoretical cross-sections for the reaction $^{51}\text{V}(n, \gamma)^{52}\text{V}$ over the continuous neutron energy up to 4 MeV using EMPIRE and TALYS-1.2 nuclear model codes. It clearly indicates that the present experimental results are in fair

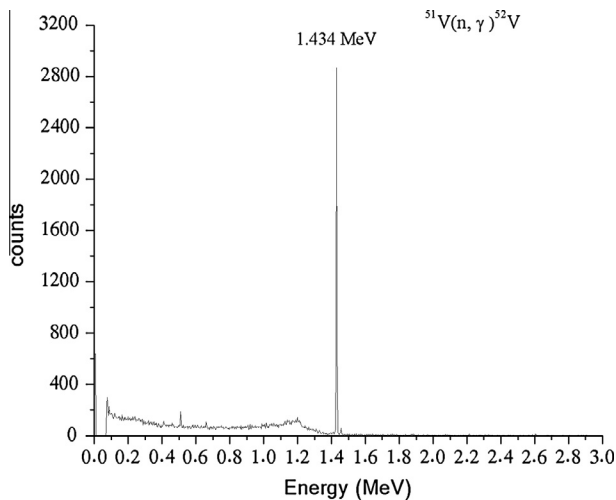


Fig. 7. Gamma-ray spectrum of ^{52}V produced through $^{51}\text{V}(n, \gamma)^{52}\text{V}$ reaction induced by continuous neutron energy.

agreement with literature data of Dudey et al. (1969), ENDF/B-VII.1 (2011), Johnsrud et al. (1959), Stavisskii et al. (1962), and Zaikin et al. (1967) and EMPIRE results. However, the TALYS-1.2 results did not show any coherence.

From the decay scheme shown in Fig. 9, it is observed that ^{128}I with half-life 24.99 min has β^- , electron capture (EC) and β^+ decays. According to the decay scheme of ^{128}I illustrated, the electrons are released in 93.1% of the ^{128}I decays through three channels to three different energy levels of ^{128}Xe . ^{128}Xe nuclei can decay from the positive parity energy level of 0.528 MeV (2+) to a metastable state 0.441 MeV (2+) with gamma emission. Moreover, ^{128}Xe nuclei can also decays from the positive parity metastable state 0.441 MeV (2+) to stable by gamma emission involving E2 transition. Similarly, electrons are released in 6.9% of the ^{128}I decays through one channel to energy level of ^{128}Te . ^{128}Te nuclei can decay from the positive parity metastable state of 0.743 MeV (2+) to stable by gamma emission involving E2 transition with half-life 3 ps. Fig. 10 shows a gamma-ray spectrum of the ^{127}I irradiated with continuous neutron energy up to 4 MeV in which photo-peaks at 0.441 MeV, 0.528 MeV, 0.743 MeV and 0.969 MeV respectively are clearly observed. These results, therefore, indicate that ^{128}I can be produced through $^{127}\text{I}(n, \gamma)^{128}\text{I}$ reaction induced by continuous neutron energy up to 4 MeV.

Fig. 11 shows measured and calculated cross-sections for $^{127}\text{I}(n, \gamma)^{128}\text{I}$ reaction, using EMPIRE and TALYS-1.2 nuclear model codes. It is observed from the figure that the present experimental result is close to the EMPIRE, than the TALYS-1.2 and other literature

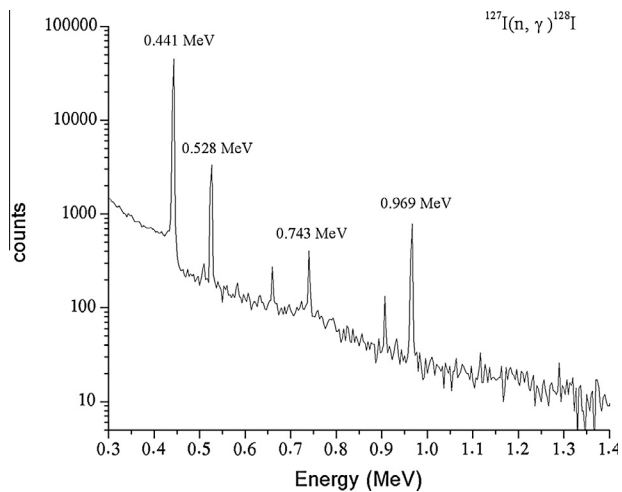


Fig. 10. Gamma-ray spectrum of ^{128}I produced through $^{127}\text{I}(n, \gamma)^{128}\text{I}$ reaction induced by continuous neutron energy.

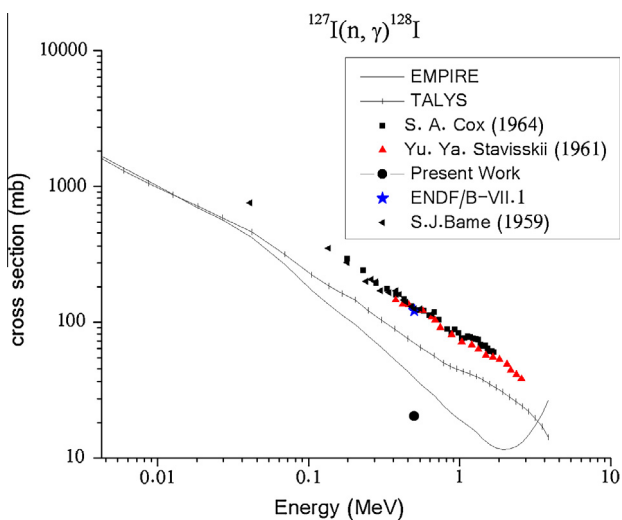


Fig. 11. Measured and calculated cross-sections for $^{127}\text{I}(n, \gamma)^{128}\text{I}$ reaction using EMPIRE and TALYS.

data. The simulated results are also obtained on the basis of best possible chosen parameters of TALYS-1.2 and EMPIRE.

Almost in all the literatures data of Bame et al. (1959), ENDF/B-VII.1 (2011), and Staviskii et al. (1962), the different energies of neutron have been produced through $^7\text{Li}(p, n)^7\text{Be}$ and $^3\text{T}(p, n)^3\text{He}$ reactions, initiated by proton beam from a Van de Graaff accelerator and measured the total cross section. Whereas in the present experiment, an electron accelerator based neutron source has been used to measure the cross section at a continuous spectrum of neutron energy.

6. Conclusion

In this study, the reaction cross sections of $^{127}\text{I}(n, \gamma)^{128}\text{I}$, $^{23}\text{Na}(n, \gamma)^{24}\text{Na}$ and $^{51}\text{V}(n, \gamma)^{52}\text{V}$ reactions for iodine, sodium and vanadium have been measured using 6 MeV electron accelerator based neutron source. The above cross-sections have been also calculated theoretically using computer code TALYS-1.2 and EMPIRE and compared with the experimental values. It is observed that the

experimental cross section for iodine, sodium and vanadium are in good agreement with the TALYS-1.2 and EMPIRE nuclear codes. The level density parameters and the adjusted value of the effective imaginary potential as input parameters to the TALYS-1.2 and EMPIRE nuclear model codes could yield cross section values close to the corresponding experimental values. The (n, γ) reaction for ^{128}I , ^{24}Na and ^{52}V have been experimentally measured and determined with relatively small uncertainties using the latest decay data. These new sets of measured data can help in fixing statistical model parameters to understand the type of reaction in terms of statistical models and to a better evaluation in the range of neutron energies from 1 keV to 4 MeV.

References

- Asgekar, V.B. et al., 1980. Single cavity 8 MeV race track microtron. *Pramana* 15 (5), 479–493.
- Bame, S.J. et al., 1959. (n, γ) cross section of ^{23}Na , ^{127}I , and ^{197}Au . *Physical Review* 113, 256–258.
- Benczer, N., Farrelly, B., Koerts, L., Wo, C.S., 1956. Investigations of ^{128}I . *Physical Review* 101, 1027–1030.
- Bhoraskar, V.N., 1988. The microtron: a recirculating electron accelerator. *Indian Journal of Physics* 62A (7), 716.
- Brink, D.M., 1957. Individual particle and collective aspects of the nuclear photoeffect. *Nuclear Physics* 4, 215–220.
- Capote, R. et al., 2009. RIPL – Reference Input Parameter Library for calculation of nuclear reactions and nuclear data evaluation. *Nuclear Data Sheets* 110, 3107.
- Curtiss, L.F., 1969. Introduction to Neutron Physics. Van Nostrand, Princeton, NJ.
- Dicksic, M., Lee, J.K., Taffe, I., Inorg, I., 1976. A search for an isomer of ^{128}I . *Nuclear Chemistry* 38, 365–366.
- Dudey, N.D. et al., 1969. Fast neutron capture by vanadium and titanium. *Journal of Nuclear Energy* 23, 443–456.
- ENDF/B-VII.1, 2011. Nuclear Data for Science and Technology: Cross Sections, Covariances, Fission Product Yields and Decay Data.
- Goriely, S., Hilaire, S., Koning, A.J., 2008. Improved microscopic nuclear level densities within the HFB plus combinatorial method. *Physical Review C* 78, 064307.
- Hauser, W., Feshbach, H., 1952. The inelastic scattering of neutrons. *Physical Review* 87, 366–373.
- Hoering, A., Weidenmuller, H.A., 1992. Gamma emission in precompound reactions. I. Statistical model and collective gamma decay. *Physical Review C* 46, 2476–2492.
- Ignatyuk, A.V., Istekov, K.K., Smirenkin, G.N., 1979. The role of collective effects in the systematics of nuclear level densities. *Journal of Nuclear Physics* 29, 450.
- Johnsrud, A.E. et al., 1959. Energy dependence of fast-neutron activation cross section. *Physical Review* 96, 951.
- Kalbach, C., 1986. Two-component exciton model: Basic formalism away from shell closures. *Physical Review C* 33, 818.
- Koning, A.J., Delaroche, J.P., 2003. Local and global nucleon optical models from 1 keV to 200 MeV. *Journal of Nuclear Physics* A713, 231–310.
- Koning, A.J., Hilaire, S., Duijvestijn, M., 2004. TALYS user manual.
- Maruyama, Y., Idenawa, K., 1967. Production of ^{128}I by small research reactor. *Journal of Nuclear Science and Technology* 4, 565–569.
- Moriyama, K., Tashiro, S., Chiba, N., Hirayama, F., Maruyama, Yu., Nakamura, H., Watanabe, A., 2010. Experiments on the release of gaseous iodine from gamma-irradiated aqueous CsI solution and influence of oxygen and methyl isobutyl ketone (MIBK). *Journal of Nuclear Science and Technology* 47, 229–237.
- Patil, B.J. et al., 2010. Simulation of e- γ -n targets by FLUKA and measurement of neutron flux at various angles for accelerator based neutron source. *Annals of Nuclear Energy* 37, 1369–1377.
- Rustgi, M.L., Lucas, J.G., Mukharjee, S.N., 1968. Application of intermediate-coupling unified nuclear model to odd-mass iodine isotopes. *Journal of Nuclear Physics* 117A, 321–335.
- Schaller, L.A., Kern, J., Michaud, B., 1971. Study of the reaction $^{127}\text{I}(n, \gamma)^{128}\text{I}$. *Journal of Nuclear Phys.* 165A, 415–432.
- Staviskii, Yu., Ya., et al., 1962. The fast neutron radiative capture cross section of ^{127}I . *Journal of Nuclear Energy. Parts A/B. Reactor Science and Technology* 16, 326–327.
- Watanabe, S., 1958. High energy scattering of deuterons by complex nuclei. *Nuclear Physics* 8, 484–492.
- Yoong, M., Pao, Y.C., Rack, E.P., 1972. Systematics of (n, γ) -activated hot iodine-128 reactions in gaseous methane and halomethanes energy degradation factor. *Journal of Physics Chemistry* 76, 2685–2689.
- Zaikin, G.G. et al., 1967. Cross sections for the radiative capture of fast neutrons by Tl^{203} and V^{51} . *Atomnaya Energiya* 23, 742–744.
- Zaman, M.R., Sarkar, M.J.A., Hossain, M.A., 2011. Production of ^{128}I atoms through $^{127}\text{I}(n, \gamma)^{128}\text{I}$ reactions in some solid iodocompounds using an (241Am-Be) neutron source. *Journal Science Research* 3 (2), 357–366.